Korean J. Chem. Eng., 38(11), 2324-2331 (2021)
DOI: 10.1007/s11814-021-0882-5

pISSN: 0256-1115
eISSN: 1975-7220

Pervaporation of hydrazine/water with ethylcellulose/4A zeolite mixed matrix membranes

Uma Maheshwari Peddoddi[†], **Dilip Kumar Behara, and Suggala Venkata Satyanarayana**

Department of Chemical Engineering, JNTUA College of Engineering, Ananthapuramu, Andhra Pradesh-515002, India

(*Received 24 March 2021 • Revised 17 May 2021 • Accepted 27 June 2021*)

Abstract−Hydrazine, a hygroscopic liquid, needs to be dehydrated for its utilization as rocket propellant. The conventional processes of separation are cumbersome, as hydrazine forms an azeotrope with water apart from being explosive and highly alkaline. Pervaporation is a well-established safe, energy intensive process for separation of azeotrope mixtures. The selection of polymer for separation of hydrazine and water is of major concern as hydrazine is highly alkaline with pH of ~13.6. Ethyl cellulose (EC) polymer withstands the high pH without any physical deformation or color change. Further, to increase the permselectivity, zeolite 4A nanoparticles were incorporated into the EC polymer matrix. The major focus of the present study was synthesis of zeolite 4A nanoparticles and preparation of ethyl cellulose- zeolite 4A mixed matrix membranes (MMMs). The zeolite particles and membranes were characterized using XRD and FTIR. The characteristics of the membranes were further observed by measuring contact angles. The pervaporation results were quite promising as the total permeate flux and selectivity were 18.35 g/m^2h and 8.46 at 36 wt% of feed water concentration with the MMMs with highest zeolite loading. The performance of the MMM's was comparatively better than pristine EC.

Keywords: Hydrazine Hydrate, Pervaporation, Ethyl Cellulose, Zeolite 4A Nanoparticles, Mixed Matrix Membranes

INTRODUCTION

Hydrazine is an important inorganic chemical compound with numerous commercial applications in agrochemicals, pharmaceuticals, plastics, chemicals, automobiles, textiles, metals, and polymers [1-3]. It is useful as rocket propellant because of its high heat of combustion with high vapor pressure. Hydrazine forms an azeotrope with water at 71.5 wt% of hydrazine; however, anhydrous hydrazine is required to use it as rocket propellant. Separation of water from hydrazine by conventional separation techniques is challenging as there is strong hydrogen bonding between hydrazine and water. Moreover, both hydrazine and water are highly polar molecules [4]. Further, hydrazine vapors are explosive during distillation, thereby necessitating high energy consumption leading to increase in cost. The drawbacks of conventional processes can be surmounted by using membrane technology [5-7]. Pervaporation is one of the reliable and established processes for separating azeotrope mixtures [8], close boiling mixtures [9], isomers [10], organic-organic solvents [11]. The process requires a simple setup which need less energy and investment [12]. As explosive decomposition of hydrazine may take place while distilling at high temperature to separate hydrazine and water, pervaporation has become a notable process as it may be carried out at ambient temperature. In addition, hydrazine is highly alkaline, with strong hydrolyzing and reducing effects; hence, the selection of polymer for dehydrating hydrazine hydrate becomes very crucial as the polymers that resist such solutions are very few.

The performance of Ethyl Cellulose (EC) membrane was explored for the separation of hydrazine and water [1]. Further, EC was modified by reacting it with phenyl isocyanate in order to introduce an appropriate amount of hydrophilic and hydrophobic moieties in polymer [12]. Further the hydrophobic hydrophilic characteristics of EC were varied by blending it with different proportions of Acrylonitrile Butadiene Styrene (ABS) and EC [13]. The modified EC membranes exhibited enhanced permselectivity compared to pristine EC. Furthermore, ceramic membranes were exclusively employed for the dehydration of hydrazine derivatives [14-17]. Therefore, a combination of polymeric membranes with the ceramic/zeolite materials, i.e., mixed matrix membranes, results in synergistic features of both organic and inorganic constituents.

In case of MMMs the selection of inorganic fillers gains primary concern as the fillers enhance the membrane's mechanical strength, thus improving the polymer matrix's stability. The fillers even improve the physicochemical properties and nanoporous morphology. Extensive research was carried out using MMMs for separating several azeotrope, close boiling, heat sensitive mixtures and gaseous mixtures [18-29]. However, feeble literature is available on separation of hydrazine and water. Therefore the novelty of the present work was preparation of MMMs with EC polymer matrix and 4A zeolite nanoparticles. The major aim of the present work was to improve the permeate flux and selectivity by embedding the zeolite 4A particles into EC to enhance the hydrophilicity and crystalline nature. The increase in hydrophilicity may increase the flux, and increase in crystallinity arrests the swelling, thereby im0 proving the selectivity. In this regard MMMs were synthesized by using the prepared zeolite 4A nanoparticles. Both nanofillers and

---

[†] To whom correspondence should be addressed.
E-mail: pmahi25@gmail.com

the membranes were characterized using XRD and FTIR techniques. The contact angles were measured and sorption characteristics were estimated for the three prepared membranes. Further pervaporation experiments were conducted to understand the effect of various parameters like zeolite loading, feed water concentration, downstream side pressure, and the results were interpreted with the help of characterization studies.

EXPERIMENTAL

1. Materials

Hydrazine hydrate and commercially available ethyl cellulose (ethoxy content of 48-49%) and sodium metasilicate were purchased from Loba Chems. Sodium hydroxide and Toluene LR (99%) was procured from Sigma Aldrich. Whereas Sodium Aluminate was bought from Merck Chemical Company. Distilled water was produced in the laboratory.

2. Synthesis of Zeolite 4A Nanoparticles

The zeolite 4A was synthesized by a stepwise procedure [30] by mixing sodium aluminate and sodium silicate solutions. Initially, aqueous sodium hydroxide solution was prepared by dissolving 4.87 g sodium hydroxide in 76 ml of distilled water and separated into two equal volume fractions. Sodium aluminate of 6.23 g was added to one fraction and sodium silicate of 16.57 g was added to another fraction to prepare aluminate and silicate solutions, respectively. Later, silicate solution was added to aluminate solution and mixed thoroughly till a homogeneous thick gel was obtained, at a pH 12. The gel was crystallized by autoclaving at 16 PSI and 120 °C for 20 min. Later the solution was cooled and separated crystal mass was dried in hot air oven, followed by calcination at 600 °C for 1 h in muffle furnace, and the obtained zeolite 4A particles were collected and stored in a sample vial for further use.

3. Synthesis of Mixed Matrix Membrane

Known weight of zeolite 4A nanoparticles (4 and 5 wt% based on the EC polymer weight) was disseminated in toluene and the mixture was ultra-sonicated for 3 h to get uniform dispersion of the particles. To this mixture ethyl cellulose polymer (6 wt%) was added and stirred at 500 rpm for 4 h to obtain a homogeneous solution. To remove the air bubbles present, the solution was left overnight and the bubble-free solution was cast on a clean glass plate. The casted membranes were dried at room temperature (~30 °C) for 24 h to vaporize the solvent completely and were named as EC4

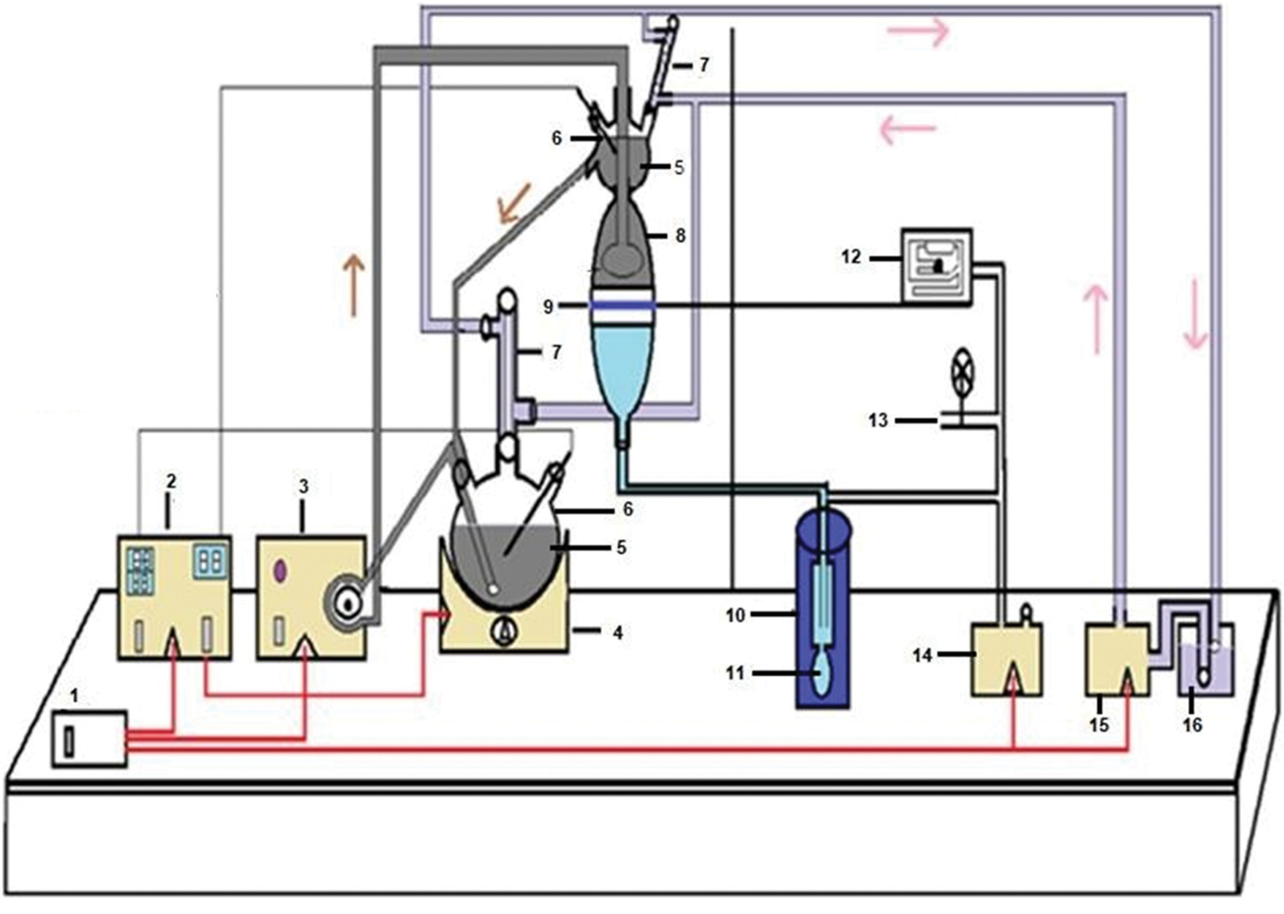

Fig. 1. Schematic diagram of experimental setup for pervaporation process.

1. Power supply
2. PID controller
3. Peristatic pump
4. Heating mantle
5. Feed solution
6. Feed container
7. Condensor
8. PV cell
9. Membrane
10. Dewar flask
11. Permeate
12. Mcleod guage
13. Needle valve
14. Vacuum pump
15. Water circulating pump
16. Cold water

and EC5, respectively. Pure ethyl cellulose membranes were prepared by dissolving 6 wt% of polymer in toluene, adopting similar procedure as above and named as EC.

4. Characterization

The morphology of zeolite 4A, EC, EC4, EC5 mixed matrix membranes was known with XRD (WRD PAN Analytical "XPERT^{3-} PRO" Germany). A CuKα source with a wavelength generation of 1.54 A^{o} was used to generate X-ray diffractogram data. Similarly, FTIR spectra recorded with Nicolet-740, Perkin-Elmer 283B IR Spectrometer, Japan, within a wavelength range of 4,000-500 cm^{-1} using KBr pellets. Further, the contact angles of water on the membranes were measured at 30 °C with sessile drop method with an Automatic Contact Angle Meter (Model CA-VP (Kyowa Interface Science Co., Japan).

5. Sorption Studies

Sorption studies were carried out to determine the sorption behavior of the polymer matrix. The synthesized membranes were cut into small pieces and weighed using five decimal Sartorius balance. The sample pieces were soaked in hydrazine/water mixture at room temperature (~30 °C) for 48 h to attain equilibrium. The samples were wiped with tissue immediately to get rid of the adhered solution and the wet weight of the membrane was measured. The difference between the wet and dry weights with respect to the dry weight of the membrane is represented as the % sorption.

6. Pervaporation Module

Pervaporation studies were carried out with EC, EC4, EC5 membranes in an indigenously made pervaporation setup as shown in Fig. 1. The pervaporation cell was of glass make with exclusively designed flanges to fix the membrane. The effective area and thickness of the membrane was 50.28 cm^{2} and ~50 μm, respectively. The pervaporation experiments were carried out at 30 °C, which was maintained constant using PID controller (Vacu Tech systems Peenya, Bangalore, Bangalore). The feed solution was circulated into the pervaporation cell using a peristatic pump and vacuum was applied using a rotary vacuum pump (Model - VTS 250, Vacu Tech systems Peenya, Bangalore) after 2 h to attain the equilibrium sorption. The pressure at the feed side was maintained at 1 atmosphere, while at the permeate side the pressure was controlled with a needle valve and measured with a McLeod gauge. Permeate was collected in a cold trap placed in Dewar flasks filled with liquid nitrogen. After 6 h of operation the Dewar flask was taken out from the setup and the cold trap was brought to room temperature and the condensed permeate was weighed and analyzed. All the experiments were repeated with a minimum of three independent readings under identical conditions of feed composition, downstream pressure and temperature to confirm the steady-state pervaporation. The percent error values in computing different mixture compositions were less than 5%.

7. Analysis

A digital refractometer (Rudolph Research Analytical DSR-k with a display resolution of 0.0001 and an accuracy of ±0.0001 at 20 °C, India) was utilized to analyze the feed sample and permeate sample of hydrazine/water system. Calibration plot of standard refractive index (RI) curve of hydrazine/water system shown in Fig. 2 was used to identify the constitution of unknown permeate samples to calculate the flux and selectivity. The performance of the synthesized membranes in separating the components of the feed mixture was thus evaluated depending on the flux and selectivity values.

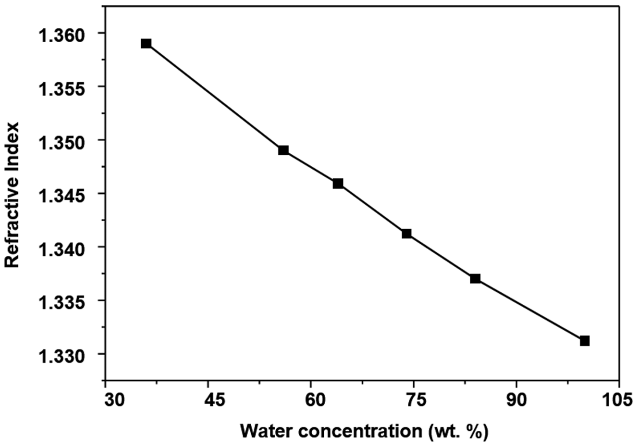

Fig. 2. Standard refractive index plot for hydrazine-water.

$$\text{Flux } J=\frac{W}{At}\ \text{g/m}^2\text{h} \tag{1}$$

where W denotes the weight of permeate collected (g), A membrane area (m^{2}), t the time of pervaporation process (h).

$$\text{Selectivity } \alpha_{wh}=\frac{x_h * y_w}{x_w * y_h} \tag{2}$$

where x, y denote weight fractions of feed and permeate and the subscripts w and h represent water and hydrazine, respectively.

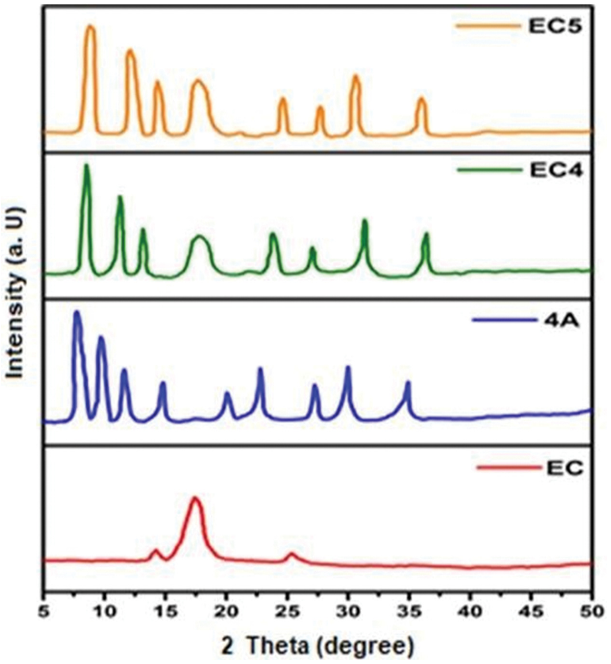

Fig. 3. XRD spectra of EC, 4A zeolite nanoparticles, EC4 and EC5 membrane.

RESULTS AND DISCUSSION

1. XRD

The X-ray diffraction spectra of EC, zeolite 4A nanoparticles, EC4, EC5 membranes are shown in Fig. 3. The pristine EC membrane showed three characteristic sharp peaks at 14°, 17°, 25.9° of 2θ [12], thus revealing that EC may be semi-crystalline. The zeolite 4A nanoparticles showed intense peaks at 2θ of 7°, 10°, 24°, 27°, pointing out the high crystalline nature of synthesized nanoparticles [19]. A slight shift in position of the characteristic peaks of EC was observed when 4A zeolite nanoparticles were incorporated into the polymer and the same was reported in literature [26]. Further, a comparative increase in sharpness of the peaks was observed for both EC4 and EC5 polymers with the increase in the wt% of the fillers as compared to plain EC, which may be due to the distribution of 4A zeolite particles into the mixed matrix membranes [30,31]. The changes thus noticed suggest that the EC4, EC5 membranes are crystalline compared to EC membrane, which may increase the selectivity.

2. FTIR

The FTIR spectra of zeolite 4A, EC, EC4 and EC5 membranes are as shown in Fig. 4. The FTIR spectra for pure EC membrane show several characteristic peaks. The peak at 3,500 cm^{-1} corresponds to the surface hydroxyl (OH) groups of EC. The peaks at 1,300 and 1,350 cm^{-1} correspond to the -CH_2 bending vibrations. The peaks at 1,650 and 1,730 cm^{-1} represent the bending of -OH groups. The peaks between 2,000 and 2,250 cm^{-1} correspond to -CH stretching vibrations. Further, the FTIR spectra peaks of zeolite confirm the presence of Si-O or Al-O and sorbed water as per reported literature [32]. Additionally, the water present in zeolite is marked with the characteristic OH stretching vibrations observed at 1,654 and 3,446 cm^{-1}, respectively. The C=C, Si-O and Al-O bonds in the zeolite 4A were marked with peaks at 1,650 cm^{-1}, 1,000 cm^{-1} and 600 cm^{-1} respectively [33]. The peaks of the MMMs EC4, EC5 coincide with the EC membrane. An increase in the intensity of the peaks can be noticed with increase in zeolite wt%.

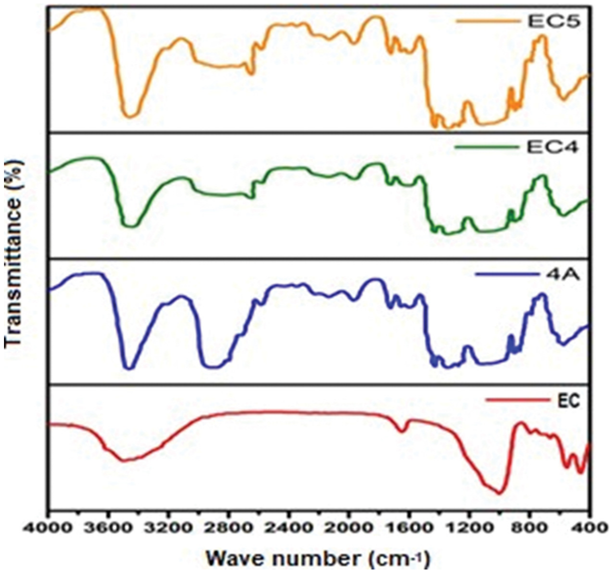

Fig. 4. FTIR spectrums of EC, 4A zeolite nanoparticles, EC4 and EC5 membrane.

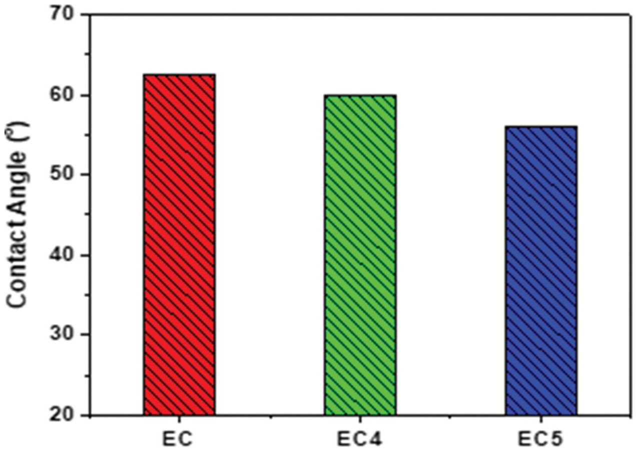

Fig. 5. Contact angles of EC, EC4 and EC5 membranes.

3. Contact Angle

The measurement of contact angle may provide the characteristic nature of the membranes. A decrease in contact angle represents increase in hydrophilic nature of the membrane. The water contact angles of EC, EC4, EC5 membranes were measured and the results are presented in Fig. 5. Contact angle of water on EC5 was found to be lower than that for EC4 membrane, which in turn was smaller than plain EC. The 4A zeolite particles are hydrophilic and the incorporation of these particles in polymer matrix has increased the hydrophilic nature of the mixed matrix membranes. Further, as expected increase of zeolite loading increased the hydrophilicity of membranes.

4. Sorption Studies

Sorption studies were carried out to understand the membrane performance. The sorption capacity of the membrane significantly influences the PV results. The extent of sorption may enhance the permeation flux. Moreover, the effect of varying wt% of zeolite

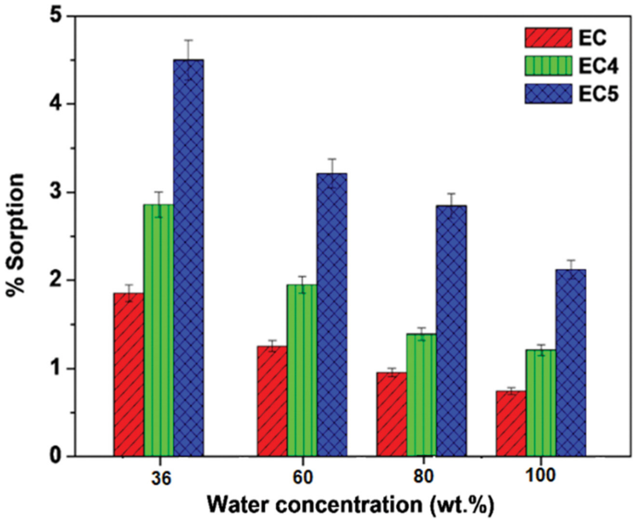

Fig. 6. Effect of zeolite 4A particles on sorption of EC, EC4 and EC5 membranes.

particles in the membrane on the sorption is measured as a function of water concentration in the hydrazine-water mixture and the obtained results are shown in Fig. 6.

As water concentration increased from 36 to 100 percent, the percentage sorption decreased from 1.854% to 0.745% for pure ethyl cellulose membrane. This may be due to the greater affinity of hydrazine to EC compared to water, and similar observations were made which affirmed that the affinity of hydrazine to EC is more than that of water. Further, the Flory-Huggins interaction parameters for hydrazine and water are 1.84 and 2.54 with EC [35]. Therefore, hydrazine is having more affinity with EC than water. Similar results were reported in literature [12,13] where the sorption of hydrazine was greater than water. However, the incorporation of the zeolite particles increased the sorption compared to plain EC. Percent sorption increased with increase in zeolite loading for given water concentration. This may be attributed to the fact that the hydrophilic nature of the membranes increased with increase in zeolite loading as explained in section 3.3.

5. Pervaporation Results

Pervaporation studies were carried out to understand the behavior of mixed matrix membranes for separating hydrazine and water. The effect of zeolite loading, water concentration and downstream side pressure was studied on permeate flux and selectivity. The experimental results are explained in section 5-1. to 5-3.

5-1. Zeolite Loading

The effect of zeolite loading in EC polymer on pervaporation flux and selectivity was studied at 64 wt% of hydrazine, at room temperature (30 °C) and downstream side pressure of 1 mmHg, respectively, and the results are shown in Fig. 7. The results for plain EC membrane are in agreement with the values reported in literature [1,2,12,34]. The low value of the selectivity may be explained due to polar-polar interactions of both hydrazine and water with EC. Further, as zeolite loading was increased from 0 to 5 wt% of the polymer, both total permeate flux and selectivity were increased from 9.896 to 26.707 g/m^{2}h and from 2.84 to 14.999 respectively. The increment may be attributed to the fact that the reinforcement of the zeolite particles resulted in increase of hydrophilicity and crystallinity of the MMMs, as revealed by the contact angle and XRD results discussed in section 3.3 and section 3.1. Therefore, the increase in hydrophilicity increased both water flux and hydrazine flux as water and hydrazine have similar structure and intramolecular forces. However, due to increase in crystallinity the swelling was arrested and coupling effect was reduced; therefore, the increase in water flux was more compared to hydrazine flux. Further, it may be reported that the kinetic diameter and molecular weight of water are smaller (diameter=3.106 Å and MW=18 g/mol) compared to hydrazine (diameter=3.7565 Å and MW=32.05 g/mol); consequently, diffusivity of hydrazine through the MMMs was less compared to water. Similar observations were reported in the literature [1,12,13]. In addition to this as the vapor pressure of hydrazine is less than that of water it enables easy desorption of water compared to hydrazine. All these factors might have resulted in increment of selectivity.

5-2. Effect of Water Concentration

The effect of feed water concentration (36 to 80 wt%) on the flux and selectivity of the membranes was studied at constant membrane thickness of ~50 μm, temperature of 30 °C and downstream side pressure of 1 mmHg, respectively. Fig. 8 depicts the effect of feed water concentration on flux for all three membranes. It may be observed from Fig. 8 that water flux increased with increase in feed water concentration. Further, at given concentration the MMMs are having higher flux compared to plain membrane. As explained in section 3.5.1, incorporation of zeolite 4A particles increased the hydrophilicity of the membrane and hence flux.

The variation of selectivity with feed water concentration is shown in Fig. 9. As expected, pervaporation selectivity increased with increase in feed water concentration for all three membranes. Further, MMMs exhibited higher selectivity compared to plain EC, and also increase in zeolite 4A concentration in the membrane is increasing the selectivity. For plain EC increase in selectivity (1.896 to 4.3) is marginal with water concentration of 36 to 80 by wt. of water. This may be due to the decrease in sorption with increase in water concentration as noticed in section 3.4 and can be ascer-

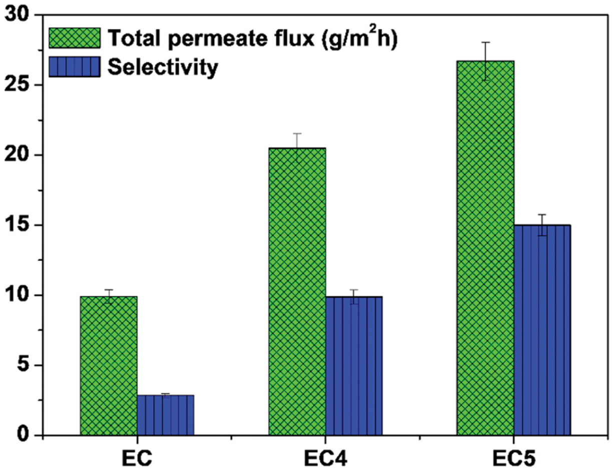

Fig. 7. Effect of zeolite loading (wt%) on total permeate flux & selectivity at 64 wt% of hydrazine, at room temperature (30 °C) and downstream side pressure of 1 mmHg.

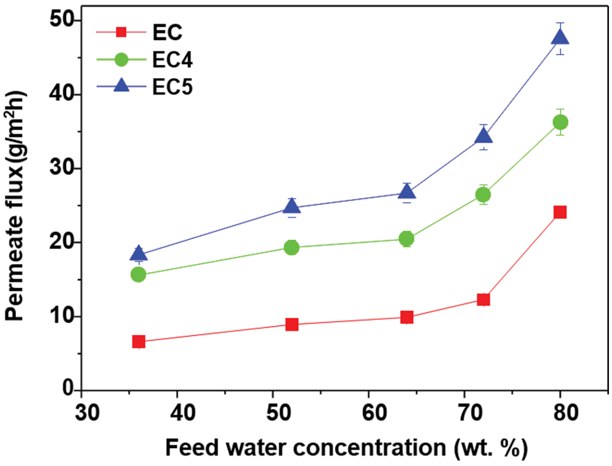

Fig. 8. Effect of feed water concentration (wt%) on permeate flux at constant membrane thickness of ~50 μm, temperature of 30 °C and downstream side pressure of 1 mmHg.

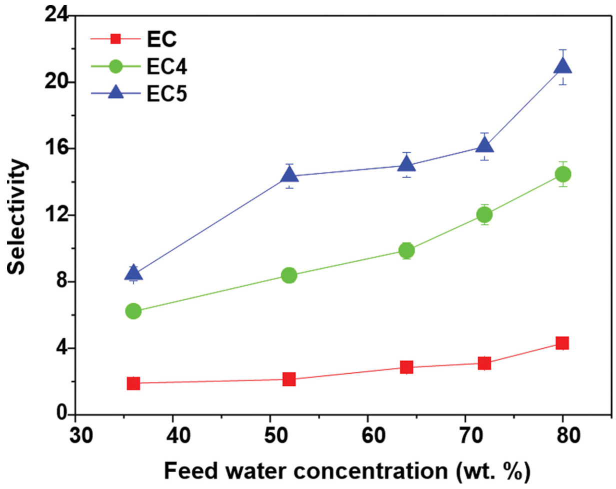

Fig. 9. Effect of feed water concentration (wt%) on selectivity at constant membrane thickness of ~50 μm, temperature of 30 °C and downstream side pressure of 1 mmHg.

tained as the affinity of hydrazine is more to EC rather than water so the sorption decreased with increase in water concentration. The sorption results reported in the present study are in agreement with that reported in literature [35], where the % sorption of water (3.5) was much less than hydrazine (7.5), indicating that water has less sorption. Further, water being the smaller molecule diffuses at a faster rate; therefore, the flux increased with increase in water concentration. Since flux is a combination of sorption and diffusion, the governing term in flux being diffusion, the water flux and thereby the total flux increased with increase in water concentration. This result is in agreement with the report that diffusion of water through EC membrane ($D_1=2.57\times10^{-8}$ cm^2/s) was greater than that of hydrazine ($D_2=0.28\times10^{-8}$ cm^2/s) [35]. Similar observations were reported in the literature wherein EC had more affinity with hydrazine compared to water, but the pervaporation flux of water was more compared to hydrazine [12]. Further, water being the smaller molecule compared to hydrazine diffuses at faster rate and diffusion selectivity contributes more to the pervaporation selectivity. The selectivity has increased by almost two-fold (6.21 to 14.469) and three-fold (8.46-20.89) for EC4, EC5, respectively, when feed water concentration changed from 36 to 80 wt%. The increase in selectivity with feed water concentration may be due to increase in crystalline nature of the membrane with addition of zeolite 4A that reduced the swelling and, hence coupling effect. It may be observed in section 3.4 the sorption selectivity (percentage sorption of pure water to percentage sorption of hydrazine hydrate) for plain EC is 0.63, whereas for EC5 is 0.52, resulting in low swelling. Further, the 4A zeolite particles allow the permeation of water and restrict hydrazine.

The performance of the synthesized pristine EC and mixed matrix membranes to separate hydrazine/water was compared with the available literature and tabulated in Table 1. The normalized flux based on 5 μm was calculated for all the reported flux values, considering the inverse relationship between flux and membrane thickness. Further, the other operating parameters, temperature T (°C), downstream pressure, P (mm Hg) and water concentration in feed mixture, F_w (wt%) are included in the table to provide an insight into the results obtained. The total permeate flux of the mixed matrix membranes of the present work is comparable with the literature values [1,12,13,33,34], where the commercial poly-

Table 1. Comparison of the pervaporation performance of MMMs with the literature data

Membrane	Normalized flux (g/m^2h for 5 μm)	Selectivity	# Other conditions T, P, F_w	Reference
EC	50.00	2.82	T=28; P=0.1; F_w=36	1
EC	96.50	1.72	T=50; P=0.1; F_w=36	12
MEC4	40.90	3.23		
PERVAP 2200	61.20	1.09		
PERVAP 2201	2.00	3.58		
PERVAP 2202	15.70	1.93		
PS	11.50	5.45		
ABS	78.10	5.07		
EC	96.50	1.71	T=50; P=0.1; F_w=36	13
BM80	32.44	10.65		
EC	55.30	3.81	T=28; P=10; F_w=48.8	33
EC-30 wt% NaA	129.52	12.37		
EC-30 wt% NaX	115.92	9.00		
PS	68.78	9.45	T=40; P=0.5; F_w=64.5	34
PS-ABS	78.70	104.29		
PS-2 wt% TiO_2	309.30	6.69		
EC	65.89	1.89	T=30; P=1; F_w=36	Present work
EC-4 wt% NaA	156.20	6.21		
EC-5 wt% NaA	183.52	8.46		

Other conditions: Feed Temperature T (°C), Downstream Pressure P (mm Hg) and water concentration in feed mixture F_w (wt%)

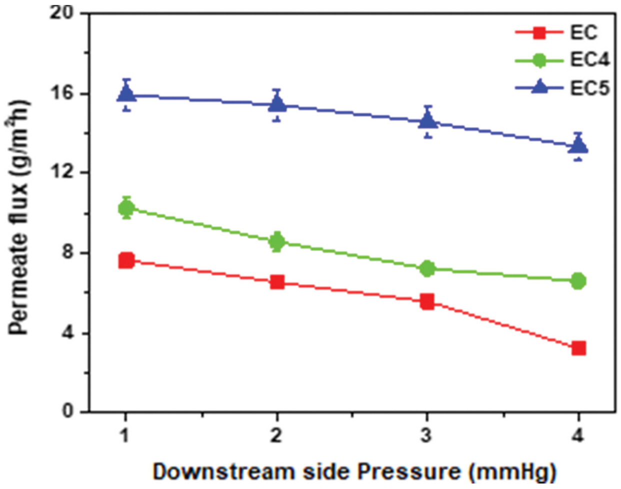

Fig. 10. Effect of downstream side pressure (mmHg) on permeate flux at constant membrane thickness of 50 μm at a temperature of 30 °C and at feed hydrazine concentration of 64 wt%.

mer, modified blend membranes and MMMs were used for pervaporation.

5-3. Downstream Side Pressure

The effect of downstream side pressure on the separation of hydrazine and water using EC, EC4, EC5 membranes was studied. The permeate side pressure was varied from 1 to 4 mmHg at constant membrane thickness of 50 μm at a temperature of 30 °C and at feed hydrazine concentration of 64.0 wt%. The variation of flux with downstream pressure is shown in Fig. 10. The results clearly show that as the downstream side pressure increases, the permeation flux decreases for all three membranes. This may be ascribed to the decrease in the driving force for permeation with increase in downstream side pressure. This is in accordance with Fick's law, which states that as the downstream side pressure increases, the permeant activity increases, thereby decreasing the activity gradients and thus decreasing the flux.

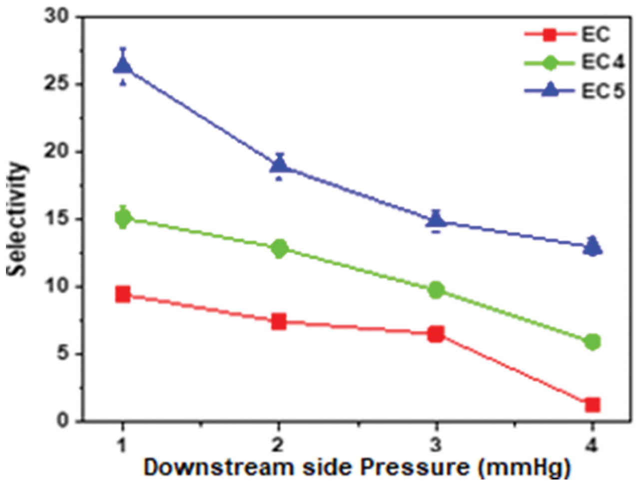

Fig. 11. Effect of downstream pressure (mmHg) on selectivity at conditions at conditions at constant membrane thickness of 50 μm at a temperature of 30 °C and at feed hydrazine concentration of 64.0 wt%.

The effect of downstream side pressure on pervaporation selectivity is shown in Fig. 11. Selectivity decreased with increase in downstream pressure for all the three membranes. The variation is more for EC5 membranes compared to other two membranes. The selectivity decreased from 26.3 to 14.21 for EC 5, whereas for EC it was 9 to 1.4 when downstream side pressure was increased from 1mm Hg to 4 mmHg. The effect of downstream side pressure on water flux is more compared to hydrazine flux and hence selectivity decreased with increase in downstream pressure.

CONCLUSIONS

MMMs consisting of EC, zeolite 4A were prepared by varying the zeolite content for separation of hydrazine and water. Hydrothermal synthesis process was used to prepare zeolite 4A particles. The XRD spectra revealed that crystallinity increased by incorporation of 4A zeolite particles into the MMMs. The FTIR spectra revealed no physical interaction between EC and zeolite. Contact angle measurements showed that hydrophilicity of MMMs is more compared to plain EC membranes. Sorption studies revealed that the percent sorption decreased with increase in water concentration and the percent sorption is more for MMMs compared to plain EC at fixed concentration. Both pervaporation flux and selectivity increased with increase in zeolite content and feed water concentration, whereas increase in downstream side pressure decreased both selectivity and flux. The outcomes of the present article will not only help to understand the mechanism of separation of components by MMMs, but also necessitate to explore MMMs for potential separation applications of industrial importance.

ACKNOWLEDGEMENTS

The authors gratefully acknowledge financial support from Department of Science & Technology (DST)-Science and Engineering Research Board (SERB), New Delhi with project file No: EMR/2017/002355.

REFERENCES

1. R. Ravindra, S. Sridhar and A. A. Khan, *J. Polym. Sci. Part B Polym. Phys.*, **37**, 1969 (1999).
2. R. Ravindra, S. Sridhar, A. A. Khan and A. K. Rao, *Polymer*, **41**, 2795 (2000).
3. M. George, K. S. Nagaraja and N. Balasubramanian, *Anal. Lett.*, **40**, 2597 (2007).
4. R. Q. Wilson, H. P. Munger and J. W. Clegg, *Chem. Eng. Prog. Symp. Ser.*, **3**, 115 (1952).
5. F. Wolf, P. Pollandt and R. Helmer, *Z. Chem. Abstr.*, **83**, 183856 (1975).
6. R. Rautenbach and R. Albrecht (Eds.), *Membrane processes*, Wiley, Chichester, UK, 368 (1989).
7. A. Duggal and E. V. Thompson, *J. Membr. Sci.*, **27**, 13 (1986).
8. G. H. Koops, J. A. M. Nolten, M. H. V. Mulder and C. A. Smolders, *J. Membr. Sci.*, **81**, 57 (1993).
9. M. Wessling, U. Werner and S.-T. Hwang, *J. Membr. Sci.*, **57**, 257

(1991).
10. B. Cao, H. Hinode and T. Kajiuchi, *J. Membr. Sci.*, **156**, 43 (1999).
11. X. Feng and R. Y. M. Huang, *Ind. Eng. Chem. Res.*, **36**, 1048 (1997).
12. S. V. Satyanarayana and P. K. Bhattacharya, *J. Membr. Sci.*, **238**, 103 (2004).
13. M. K. Mandal, S. Dutta and P. K. Bhattacharya, *Chem. Eng. J.*, **138**, 10 (2008).
14. M. Kazemimoghadam, P. Afshin and T. Mohammadi, *Micro. Meso. Mater.,* **70**, 127 (2004).
15. M. Kazemimoghadam and T. Mohammadi, *Desalination*, **262**, 273 (2010).
16. M. Kazemimoghadam and T. Mohammadi, *Sep. Purf. Technol.*, **47**, 173 (2006).
17. M. Kazemimoghadam and T. Mohammadi, *Iranian J. Mater. Sci. Eng.*, **8**, 1 (2011).
18. J. P. Boom, D. Bargeman and H. Strathmann, *In Studies in Surf. Sci. and Catal.*, **84**, 1167 (1994).
19. M. Sairam, M. B. Patil, R. S. Veerapur, S. A. Patil and T. M. Aminabhavi, *J. Membr. Sci.*, **281**(1-2), 95 (2006).
20. D. Hua, Y. K. Ong, Y. Wang, T. Yang and T. S. Chung, *J. Membr. Sci.*, **453**, 155 (2014).
21. R. Castro-Muñoz, F. Galiano, V. Fíla, E. Drioli and A. Figoli, *Rev. Chem. Eng.*, **35**(5), 565 (2019).
22. G. B. Thorat, S. Gupta and Z. V. P. Murthy, *Chin. J. Chem. Eng.*, **25**(10), 1402 (2017).
23. X. Wang, J. Chen, M. Fang, T. Wang, L. Yu and J. Li, *Sep. Purif. Technol.*, **163**, 39 (2016).
24. S. B. Teli, M. Calle and N. Li, *J. Membr. Sci.*, **371**(1-2), 171 (2011).
25. R. Castro-Muñoz, O. D. L. Iglesia, V. Fíla, C. Téllez and J. Coronas, *Ind. Eng. Chem. Res.*, **57**(47), 15998 (2018).
26. R. S. Murali, A. F. Ismail, M. A. Rahman and S. Sridhar, *Sep. Purif. Technol.*, **129**, 1 (2014).
27. W. Zou, H. Bai, L. Zhao, K. Li and R. Han, *J. Radioanal. Nucl. Ch.*, **288**, 779 (2011).
28. W. S. Chi, S. Hwang, S. J. Lee, S. Park, Y. S. Bae, D. Y. Ryu and J. Kim, *J. Membr. Sci.*, **495**, 479 (2015).
29. S. Hwang, W. S. Chi, S. J. Lee, S. H. Im, J. H. Kim and J. Kim, *J. Membr. Sci.*, **480**, 11 (2015).
30. J. Ahmad and M. B. Hagg, *Sep. Purif. Technol.*, **115**, 190 (2013).
31. K. Sunitha, K. Y. Rani, S. Moulik, S. V. Satyanarayana and S. Sridhar, *Desalination*, **330**, 1 (2013).
32. G. Khatinzadeh, M. Mahdyarfar and A. Mehdizadeh, *Petroleum Sci. Technol.*, **31**(13), 1313 (2013).
33. M. Norouzi, S. Ofoghi, A. Parnia-Baran and M. Rahim-Khorasani, *Int. J. Environ. Anal. Chem.*, 1 (2020).
34. S. S. Hosseini, E. Mehralian, M. H. Ekbatan and P. Li, *Korean J. Chem. Eng.*, **38**(3), 587 (2021).
35. R. Ravindra, K. R. Krovvidi, A. A. Khan and A. K. Rao, *Macromolecules*, **30**(11), 3288 (1997).